Synthesis and Spectroscopic Characterization of Bis-Pocket Porphyrins: Tetrakis(2,6-dinitrophenyl)porphyrin and Catalytic Activity of a Manganese(III) Chloride Derivative in Alkane Oxidation[†]

Carlos A. Quintana, Roger A. Assink, and John A. Shelnutt*

The synthesis of tetrakis(2,6-dinitrophenyl)porphyrin (TDNPP) and tetrakis(2,6-diaminophenyl)porphyrin (TDAPP) has been achieved by modifying the Lindsey method as described. The new porphyrins serve as percursors for the synthesis of bis-deep-pocket metalloporphyrins that have completely enclosed, but dynamically accessible, cavities located adjacent to the central metal core on both faces of the macrocycle. Proton nuclear magnetic resonance spectroscopy of TDNPP shows that the porphyrin is substituted at the two phenyl positions ortho to the methine bridge carbon of the porphyrin. Fourier transform infrared spectroscopy demonstrates that the ortho substituents of the phenyl rings are in fact NO_2 groups for TDNPP and NH_2 groups for TDAPP. The manganese(III) chloride derivative of TDNPP was also synthesized and characterized by UV–visible absorption and resonance Raman spectroscopy. The Mn derivative was found to catalyze the hydroxylation of alkanes by using iodosylbenzene as the oxidant.

Introduction

The ability of enzymes to recognize the size and shape of substrate molecules is well-known, and efforts to design synthetic catalysts with similar capabilities are under way in many laboratories. Two synthetic requirements for mimicking the remarkable capabilities of enzymes are (1) the construction of a cavity capable of substrate size and shape recognition and (2) the incorporation of the desired catalytic center into the shape selective cavity.

The metalloporphyrins provide an excellent starting point for fulfilling these synthetic requirements. First, they provide a sturdy molecular foundation upon which additional molecular architecture can be erected to construct the molecular recognition site. In fact, metalloporphyrin synthetic strategies are well developed; almost any kind and combination of peripheral substituents can be added to the macrocycle to form the desired cavity. In addition, the metal center in metalloporphyrins is known to catalyze many reactions of commercial interest, such as hydrocarbon oxidation[1,2] and dehalogenation reactions.[3]

Toward the goal of synthesizing biomimetic catalysts, a number of bis-pocket porphyrins have been synthesized and evaluated in alkane oxidation reactions that mimic cytochrome P_{450} chemistry.[4–7] The idea is to provide a cavity at the catalytic site (the heme Fe atom) that is shape and size specific for the alkane substrate of interest. Most notable among the bis-pocket porphyrins synthesized to date is tetrakis(2,4,6-triphenylphenyl)-porphinate (TTPPP).[7] This porphyrin, with its phenyl substituents at the ortho positions of the phenyl rings of tetraphenylporphyrin (TPP), provides a shallow pocket at the metal site on both faces of the porphyrin macrocycle. The regioselectivity for alkane hydroxylation shown by Mn or Fe derivatives of TTPPP is comparable to or better than that of isoenzymes of cytochrome P_{450}, which carry out primary alcohol biosynthesis.[8–10]

We are interested in constructing even deeper small cavities by adding more bulky substituents at the ortho-phenyl positions of TPP. One method is to connect bulky substituents to the phenyl rings of TPP via an amide linkage in analogy with the mono-ortho-substituted "picket-fence" porphyrins.[11] The synthesis of picket-fence porphyrin is carried out by first making the tetrakis(o-nitrophenyl)porphyrin, converting the nitro groups to the amines, and condensing the amine with the acid halide of the desired substituent to form amide links. This method has been used to prepare porphyrins with a deep pocket on one side of the porphyrin by attaching carboranes[12,13] to the α^4-tetrakis(2-aminophenyl)porphyrin precursor[12] (the α^4 notation denotes the isomer with all four amino groups oriented toward the same side of the porphyrin macrocycle).

We are using molecular modeling techniques to design deep pocket porphyrins to carry out alkane hydroxylation reactions and, from this perspective, have become interested in synthesizing deep-pocket porphyrins with pockets located on both faces of the macrocycle. The molecular modeling studies indicate at least three advantages for the *bis*-deep-pocket porphyrins over those with only one sterically hindered face. First, the reactions occurring on both faces of the macrocycle are subject to control by the presence of deep cavities, and second, dynamical calculations suggest that the macrocycle remains more planar than the α^4-porphyrins. Finally, isomerization of the ortho substituents at high temperatures is not a problem for the di-ortho-substituted tetraphenylporphyrins. Consequently, we have undertaken the synthesis of bis-deep-pocket tetraphenylporphyrin derivatives for the purpose of biomimetic oxidation of hydrocarbons.

Here, we report the synthesis of the free base tetrakis(2,6-*di*nitrophenyl)porphyrin (H$_2$TDNPP, **1**) and its conversion to the 2,6-*di*aminophenyl derivative (H$_2$TDAPP). These porphyrins serve as precursors for preparation of bis-deep-pocket porphyrins analogous to the picket-free porphyrins. H$_2$TDNPP is structurally characterized by using UV–visible absorption, proton NMR, and FTIR spectroscopy and laser desorption FT mass spectrometry. We also describe the preparation of the manganese(III) chloride derivative of TDNPP and the alkane hydroxylation activity of this bis-pocket porphyrin.
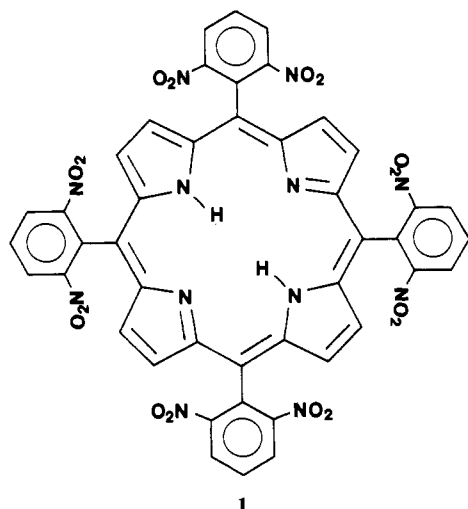
Materials and Methods

Synthesis of Tetrakis(2,6-dinitrophenyl)porphyrin Free Base. The method used to synthesize H$_2$TDNPP is based on the strategy described by Lindsey et al.[14] for synthesis of meta- and para-substituted tetra-

---

(1) Groves, J. T.; Nemo, T. E.; Myers, R. S. *J. Am. Chem. Soc.* **1979**, *101*, 1032.

(2) Tabushi, I.; Koga, N. *Tetrahedron Lett.* **1978**, 5017.

(3) Anders, M. W.; Pohl, L. R. Halogenated Alkanes. In *Bioactivation of Foreign Compounds*; Anders, M. W., Ed.; Academic: Orlando, FL, 1985; Chapter 10.

(4) Momenteau, M. *Pure Appl. Chem.* **1986**, *58*, 1493.

(5) Zipplies, M. F.; Lee, W. A.; Bruice, T. C. *J. Am. Chem. Soc.* **1986**, *108*, 4433.

(6) Woon, T. C.; Dicken, C. M.; Bruice, T. C. *J. Am. Chem. Soc.* **1986**, *108*, 7990.

(7) Cook, B. R.; Reinert, T. J.; Suslick, K. S. *J. Am. Chem. Soc.* **1986**, *108*, 7281.

(8) Frommer, U.; Ullrich, V.; Staudinger, H.; Orrenius, S. *Biochem. Biophys. Acta* **1972**, *280*, 487.

(9) Ellin, A.; Orrenius, S. *Mol. Cell. Biochem.* **1975**, *8*, 69.

(10) Morohashi, K.; Sadano, H.; Okada, Y.; Omura, T. *J. Biochem.* **1983**, *93*, 413.

(11) Collman, J. P.; Gagne, R. R.; Reed, C. A.; Halbert, T. R.; Lang, G.; Robinson, W. T. *J. Am. Chem. Soc.* **1975**, *97*, 1427.

(12) Kahl, S. B. In *Neutron Capture Therapy*; Hatanaka, H., Ed.; Mishimura: Niigata, Japan, 1986.

(13) Gabel, D.; Fairchild, R. G.; Hillman, M.; Oenbrink, G.; Muller, R. In *Neutron Capture Therapy*; Hatanaka, H., Ed.; Mishimura: Niigata, Japan, 1986; p 37, 1986.

---

*To whom correspondence should be addressed.

1

Figure 1. UV–visible absorption spectra of (a) H_2TDAPP, (b) H_2TDN-PP, (c) H_2TF_5PP, and (d) H_2TPP in methylene chloride.

phenylporphyrins. To a dry 2000-mL three neck flask were added, 1000 mL of freshly distilled and dried (from anhydrous sodium sulfate) methylene chloride, 4.8 g of 2,6-dinitrobenzaldehyde (Aldrich), and 40 g of activated 4-Å molecular sieves (Davidson). Also, 0.5 mL of 50% boron trifluoride–ethyl ether (Kodak) was added as a catalyst. A reflux condenser and a gas-discharge tube attached to a source of dry nitrogen through a rubber septum were connected to the flask. The condenser is operated at –20 °C to insure condensation of CH_2Cl_2 at the 2–3 mL/min flow rate of dry nitrogen through the solvent. Then, 2.0 mL of freshly distilled pyrrole (Kodak) in 200 mL of distilled CH_2Cl_2 was added slowly over 6 h from an addition funnel attached to the third neck of the flask. Pyrrole and dinitrobenzaldehyde condensed to form the porphyrinogen while the mixture was stirred at room temperature (23 °C) in the dark. Afterward, the porphyrinogen was oxidized to the porphyrin by the addition of 5.5 g of *p*-chloranil (tetrachloro-1,4-benzoquinone, Fisher). The reaction mixture was refluxed at 39 °C for 5 h while being stirred. During this time, the formation of the porphyrin was carefully monitored by its UV–visible absorption spectrum. Then, the reaction mixture was added to a 2000-mL flask containing 300 g of inactive (washed with methanol) alumina, and the mixture was evaporated to dryness. The powder was placed into a Büchner funnel and washed with methanol (∼1500 mL) until no UV–visible detectable material was removed. Afterward, the porphyrin was extracted from the alumina with methylene chloride. To the eluent was added 300 g of silica and the mixture evaporated to dryness. The porphyrin was extracted with CH_2Cl_2 and concentrated to 50 mL.

The concentrated porphyrin solution was purified by chromatography on a column (8 cm × 80 cm) of inactive γ-alumina (Fisher) eluted with methylene chloride. The second dark brown band contained the H_2TD-NPP. The fractions that composed this band were collected and concentrated to 50 mL. The crude porphyrin solution was further purified by chromatography on silica gel (60–100 mesh) with methylene chloride as the eluent. Again, the second band off the column was the porphyrin, which, upon drying, gave a dark purple powder. For four repetitions of the preparation the yield was 100–800 mg (2–13%).

Synthesis of (Tetrakis(2,6-dinitrophenyl)porphinato)manganese(III) Chloride. To glacial acetic acid (100 mL) in a 250-mL round-bottom flask were added 100 mg of H_2TNDPP, 1.0 g of manganese(III) chloride (Fisher), and 1.5 g of anhydrous sodium acetate (Spectrum). The mixture was refluxed for 16 h. The mixture was removed from the heat, 100 mL of water was added, and the mixture was cooled to room temperature. The mixture was extracted with five 100-mL portions of distilled chloroform. The fractions were combined and dried over anhydrous sodium sulfate to yield a dark brown powder (103 mg). The product was purified by chromatography on alumina with methylene chloride. The material quickly separated into two bands, a bright green band (eluted first) and a dark reddish brown band that contains the metalated porphyrin. The red-brown band was collected and evaporated to dryness to yield 96 mg of a dark brown powder. The metal derivative was further purified by chromatography on silica gel using first methylene chloride followed by acetone. The reddish brown band was collected and dried to yield 81 mg of a dark brownish purple material. Brown plates were crystallized from methylene chloride–hexane solution.

Synthesis of Tetrakis(2,6-diaminophenyl)porphyrin Free Base. Concentrated HCl (100 mL), 50 mg of H_2TDNPP, and 1.5 g of tin(II)
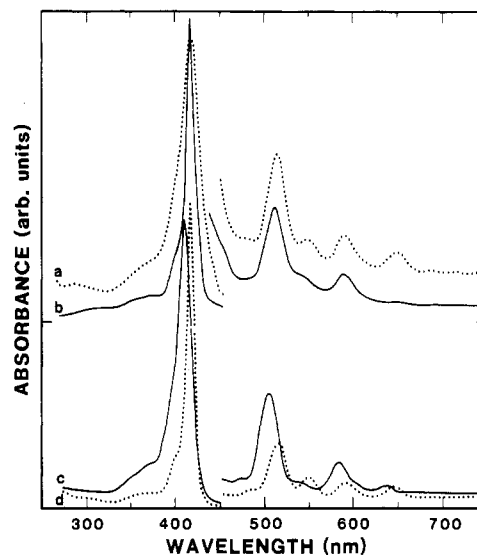
chloride (Aldrich) were added to a 250-mL round-bottom flask and heated to 68 °C for 1 h, allowed to cool to room temperature, and stirred for an additional 15 h. Slowly, 100 mL of water was added, and then the solution was slowly neutralized with a concentrated solution of NaOH. Tin hydroxide precipitated as a white material. The filtered mixture was extracted with five 100-mL portions of distilled chloroform. The fractions were combined and dried over anhydrous sodium sulfate, filtered, and evaporated to dryness. Yield was about 40 mg of a purple powder. The crude material was purified by chromatography on alumina using first methylene chloride and then acetone as the eluent. The dark brown band was collected, concentrated, and further purified by chromatography on a silica gel column. Yield was about 40 mg of a purple powder.

UV–Visible Absorption Spectroscopy. Absorption spectra were obtained by using a Perkin-Elmer Model 330 UV–visible–near-IR spectrophotometer. Samples were dissolved in methylene chloride and spectra were taken in 1-cm path length quartz optical cells maintained at 20 °C.

FTIR Spectroscopy. Infrared spectra were obtained on a Perkin-Elmer Model 1750 FTIR spectrometer. KBr pellets containing the polycrystalline porphyrins or solutions of the porphyrin in methylene chloride were used.

Resonance Raman Difference Spectroscopy. Resonance Raman spectra of $Mn^{III}TDNPP(Cl)$ in methylene chloride were obtained by using a Raman difference spectrometer whose construction was described previously.[15] Comparisons of spectra obtained simultaneously on the Raman difference spectrometer easily gives accurate (error ∼ 0.1 cm⁻¹) comparisons of the frequencies of corresponding Raman lines in the two spectra. Methylene chloride solutions of the porphyrin were placed in one of two compartments of a partitioned cylindrical cell that was spun at 50 Hz. Scattered light was collected at 90° to the incident laser beam from a krypton ion laser.

Proton NMR Spectroscopy. The ^1H NMR spectra were recorded at 199.5 MHz on a Chemagnetics rf console interfaced to a General Electric 1280 data station and pulse programmer. The 0.5-cm probe and 4.7-T magnet were purchased from Cryomagnet Systems and Nalorac Cryogenics, respectively. The sample consisted of approximately 2.0 mg of TDNPP in 0.5 mL of deuterated chloroform. The ^1H signal (7.27 ppm) of the residual undeuterated chloroform was used as a reference. Spectral simulations were performed by using the commercial General Electric 1280 software.

Mass Spectrometry. Laser desorption FT mass spectra were obtained using a Nicolet FTMS2000 mass spectrometer and a Tachisto CO_2 laser (Model 216).

Results and Discussion

Characterization of Tetrakis(2,6-dinitrophenyl)porphyrin. H_2TDNPP was structurally characterized by proton NMR, UV–visible absorption, and FTIR spectroscopy and laser desorption FT mass spectrometry. The FT mass spectra showed a parent peak at 975 amu, in good agreement with the calculated value for $C_{44}N_{12}O_{16}H_{22}$ of 974.71.

(14) Lindsey, J. S.; Schreiman, I. C.; Hsu, H. C.; Kearney, P. C.; Marguerettaz, A. M. *J. Org. Chem.* **1987**, *52*, 827.

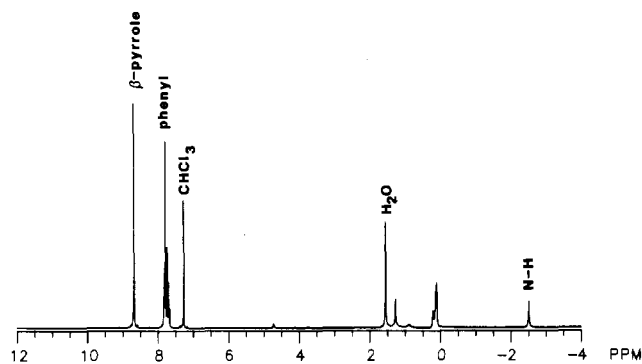(15) Shelnutt, J. A. *J. Phys. Chem.* **1983**, *87*, 605.

Figure 2. ¹H NMR spectrum of free base tetrakis(2,6-dinitrophenyl)-porphyrin in deuterated chloroform.
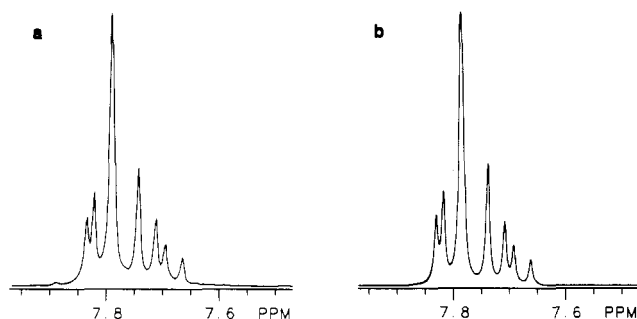

Figure 3. Experimental (a) and simulated (b) ¹H NMR spectra of the phenyl hydrogens in tetrakis(2,6-dinitrophenyl)porphyrin.

Figure 4. FTIR spectra of (a) H₂TDNP and (b) H₂TDAPP in KBr pellets.

The UV–visible absorption spectrum of H₂TDNPP is shown in Figure 1. The Soret or B band occurs at 417 nm and the $Q_y(0-1)$ and $Q_x(0-1)$ bands occur at 513 and 589 nm, respectively. These bands are vibrational satellites of the weak $Q_y(0-0)$ and $Q_x(0-0)$ that have maxima near 540 and 640 nm. The electronic properties of the nitro groups in the ortho positions account for the weakness of the 0–0 bands and the absence of the normal *etio* absorption band intensity pattern,[16] which has the Q-band intensities increasing with increasing energies of the four Q transitions. The *phyllo* type absorption spectrum is observed generally for ortho-substituted porphyrins such as tetrakis(pentafluorophenyl)porphyrin (H₂TF₅PP) (Figure 1).

The ¹H NMR spectra of H₂TDNPP in chloroform solution is shown in Figure 2. We assign the eight equivalent β pyrrole hydrogens to the resonance at 8.68 ppm, the phenyl hydrogens to the peaks in the region 7.6–8.3 ppm, and the pyrrole N–H to the resonance at –2.51 ppm. (The hydrogens of chloroform and water resonant at 7.24 and 1.55 ppm, respectively. Minor solvent impurities account for the resonances at 1.27 and 0.90 ppm.) The porphyrin assignments in Figure 2 are consistent with the chemical shifts of various diamagnetic porphyrins reported in the literature.[17] For example, the β pyrrole hydrogen resonances of H₂TPP are reported as 8.75 ppm (in chloroform), the pyrrole N–H of H₂TPP resonates at –2.07 ppm (in trifluoroacetic acid) and the meta and para phenyl hydrogen resonances of H₂TPP are observed near 7.8 ppm (in chloroform).

The assignments and the extent and location of the nitro group substitution are supported by several spectral features: (1) the ratios of the resonance integrals, (2) the increased line width of the pyrrole N–H, and (3) the analysis of the fine structure of the phenyl hydrogens. First, the experimental ratios of the integrals of resonances (from low to high field) are 8.0:12.4:2.1, in good agreement with the theoretical ratios of 8.0:12.0:2.0 for the number of β pyrrole, phenyl, and pyrrole N–H hydrogens. Second, the line widths of the resonances of the eight equivalent β pyrrole
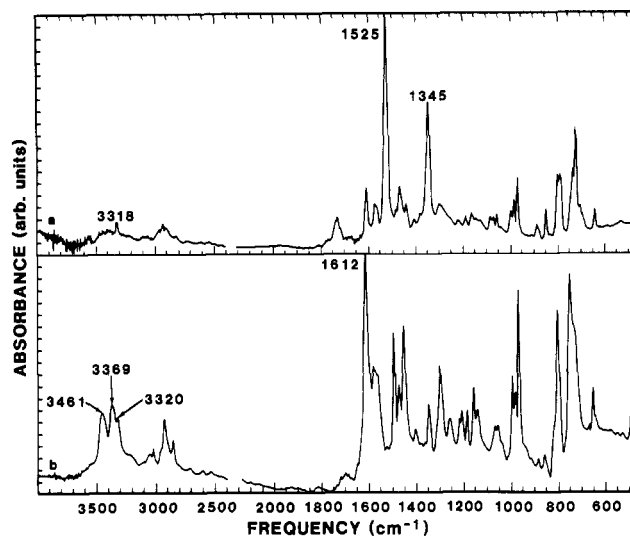
hydrogens and the phenyl hydrogens are 1.9 and 1.7 Hz, respectively, while the line width of the pyrrole N–H resonance is 5.0 Hz. The increased line width of the pyrrole N–H resonance is due to its rapid exchange with the trace amounts of water in the solvent. Finally, Figure 3a shows an expansion of the phenyl hydrogen region of the spectrum. Also shown (Figure 3b) is a spectrum simulation that assumes an AB₂ configuration with chemical shifts of 7.71 and 7.80 ppm for the A and B protons, respectively, and a coupling constant of 8 Hz. An AB₂ pattern would be expected if the phenyl group were identically substituted in either both positions ortho or both positions meta to the methine bridge carbon. The coupling of phenyl hydrogens ortho to each other ranges from 6 to 10 Hz with a usual value of 8 Hz. (In contrast, the coupling of phenyl hydrogens meta to each other ranges from 0 to 3 Hz with a typical value of 2 Hz, and the coupling of para phenyl hydrogens is from 0 to 1 Hz with a usual value of 1 Hz.)[18] Thus, the coupling constant and multiplet pattern strongly support the presence of phenyl rings substituted in both phenyl positions ortho to the porphyrin meso carbon.

The UV–visible absorption and proton NMR results demonstrate that the phenyl rings are identically substituted at the 2- and 6-positions, but do not identify the ortho substituent itself. However, the FTIR spectrum clearly shows that the porphyrin has phenyl NO₂ substituents. As can be seen in Figure 4, the symmetric and asymmetric N═O stretching vibrations at 1345 and 1525 cm⁻¹, respectively, dominate the IR spectrum of the porphyrin macrocycle and phenyl rings. These values compare favorably with 1352 and 1525 cm⁻¹ for tetrakis(2-nitrophenyl)-porphyrin, and they are well within the ranges (1320–1360 and 1490–1550 cm⁻¹) expected for aromatic nitro compounds.[19] Also, the pyrrole N–H stretching mode is observed at 3318 cm⁻¹.

Characterization of Tetrakis(2,6-diaminophenyl)porphyrin. The UV–visible absorption spectrum of H₂TDAPP is shown in Figure 1. The spectrum is almost identical with that of α⁴-H₂TAPP. The Soret band maximum at 418 nm is slightly red-shifted (1 nm) from that of the dinitro compound. The Soret band of the amino compound is also much broader than that for H₂TDNPP. The presence of the lone pair of electrons on the amino substituents causes the broadening. Inhomogeneous broadening is not expected for H₂TDNPP. The nitro and amino substituents may also affect the rotational freedom of the phenyl rings. The $Q_x(0-0)$ and $Q_y(0-0)$ band maxima occur at 650 and 549 nm and are much stronger than those for H₂TDNPP. The $Q_x(0-1)$ and $Q_y(0-1)$

(16) Falk, J. E. *Porphyrins and Metalloporphyrins*; B. B. A. Library, Vol. 2; Elsevier: Amsterdam, 1964.

(17) Janson, T. R., Katz, J. J. Nuclear Magnetic Resonance Spectroscopy of Diamagnetic Porphyrins. In *The Porphyrins*; Dolphin, D., Ed.; Academic: New York, 1979; Vol. 4. Chapter X.

(18) Atta-ur-Rahman *Nuclear Magnetic Resonance*; Springer-Verlag: New York, 1986.

(19) (a) Lambert, J. *Organic Structural Analysis*; MacMillan: New York, 1976; Chapter 4. (b) Colthup, N. B.; Daly, L. H.; Wiberley, S. E. *Introduction to Infrared and Raman Spectroscopy*; Academic: New York, 1975; Chapter 11.
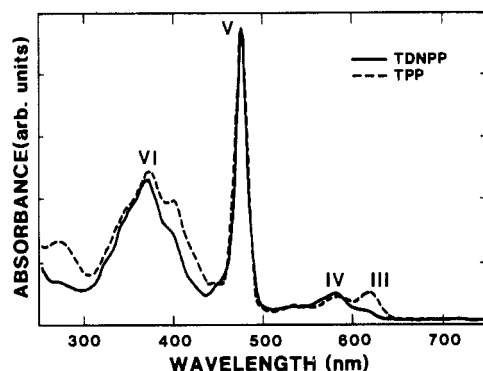
Figure 5. UV–visible absorption spectra of (- - -) $Mn^{III}TPP(Cl)$ and (—) $Mn^{III}TDNPP(Cl)$ in methylene chloride.

transitions are at 590 and 515 nm, slightly red-shifted (1 nm) from the peak wavelengths of H_2TDNPP. Thus, the *etio* pattern of band intensities is partially restored by substitution of electron-donating amines for the nitro substituents.

The FTIR spectrum of H_2TDAPP is given in Figure 4 and clearly demonstrates conversion of the nitro groups to amines. The N=O stretching vibrations disappear and are replaced by the strong NH_2 deformation mode at 1612 cm^{-1}. New lines appear at 3461 and 3369 cm^{-1} and are identified as the NH_2 stretching modes. These frequencies are in good agreement with the α^4-tetrakis(2-aminophenyl)porphyrin frequencies at 1618 for the NH_2 deformation and 3470 and 3375 cm^{-1} for the asymmetric and symmetric NH_2 stretches. The ranges for aromatic primary amines in solution are 1590–1650 cm^{-1} for the NH_2 deformation and 3420–3520 and 3325–3420 cm^{-1} for the NH_2 stretching.[19] The NH_2 stretching bands are usually broad with some structure and a shoulder near 3200 cm^{-1}.

Characterization of (Tetrakis(2,6-dinitrophenyl)porphinato)-manganese(III) Chloride. Free base TDNPP was converted to its manganese(III) chloride derivative, and the absorption and resonance Raman spectrum were obtained. The absorption spectrum of $Mn^{III}TDNPP(Cl)$ is shown in Figure 5. $Mn^{III}TD-NPP(Cl)$ shows a hyper-porphyrin[20] absorption spectrum in that strong extra absorption bands are evident and the "Soret" band, called band V, at 478 nm is abnormally shifted. The spectrum is very similar to the $Mn^{III}TPP(Cl)$ spectrum, which has bands at 375 (band VI), 477 (band V), 582 (band IV), and 618 (band III) nm. (We labeled the bands as proposed by Boucher.[21]) Although the absorption bands are in roughly the same positions for TPP and TDNPP, the intensities vary significantly. For some Mn(III) porphyrins, band V is weaker than band VI; another absorption (band V_a) is typically found between bands V and VI. It is not clear which of the spectral features is band V_a in the TPP or TDNPP spectra,[21] but V_a is probably the band near 400 nm.

The Raman spectrum of $Mn^{III}TDNPP(Cl)$ obtained with 406.7-nm excitation is shown in Figure 6 along with the spectrum of $Mn^{III}TPP(Cl)$ for comparison. The region of the Raman spectrum shown in Figure 6 contains lines sensitive to the oxidation state (macrocycle π-charge density) and core size (center-to-nitrogen$_{pyrrole}$ distance). The lines at 1362, 1456, 1497, 1559, and 1580 cm^{-1} are the core-size markers ν_4, ν_3, ν_{12}, ν_2, and ν_{11} based on the latest assignments of Parthasarathi et al.[22] These lines shift by no more than 1 cm^{-1} upon replacement of the ortho phenyl protons by NO_2 groups. The small shifts indicate a difference of no more than 0.002 Å in the core sizes of the two compounds. Most notably, ν_2 is 1.2 cm^{-1} higher for $Mn^{III}TDNPP(Cl)$ than for $MnTPP(Cl)$, with much smaller shifts for the other marker lines. Helms et al.[23] noted a correlation between the frequency
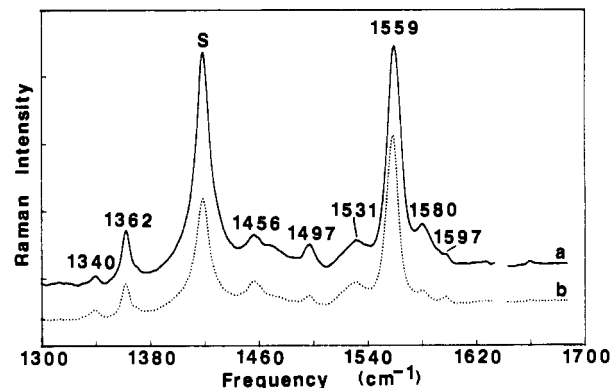

Figure 6. Resonance Raman spectra of (a) manganese(III) tetrakis-(2,6-dinitrophenyl)porphyrin chloride and (b) manganese(III) tetra-phenylporphyrin chloride in methylene chloride taken with 406.7-nm excitation.

of ν_2 and the electron-withdrawing ability of the phenyl substituents for a series of (μ-oxo)iron(III) tetraphenylporphyrin dimers. In fact, a plot of ν_2 versus $\sum\sigma$, where σ are the Hammett constants for the phenyl ring substituents, gives a good correlation ($r = 0.997$). Using the slope of the linear relationship between ν_2 and $\sum\sigma$, we would expect an increase in ν_2 of 10 cm^{-1} upon substitution of nitro groups for the ortho hydrogens of TPP—a much larger increase than the 1.2-cm^{-1} increase observed for TDNPP. Thus, the correlation may only hold for the (μ-oxo)iron dimer or may not be valid for ortho substituents.

The appearance of the ν_{20} vibration (line at 1531 cm^{-1}) demands an explanation.[22] It has been noted that ν_{20} is an anomalously polarized line resulting from an A_{2g} symmetry normal mode. In D_{4h} molecular symmetry, A_{2g} modes are resonantly enhanced in the Raman spectrum only by the Herzberg–Teller (B-term) vibronic coupling mechanism.[24-26] In contrast, the A_{1g}, B_{1g}, and B_{2g} allowed modes are enhanced by both the Herzberg–Teller (interstate) coupling mechanism and the Franck–Condon (A_{1g} modes) or Jahn–Teller (B_{1g} and B_{2g} modes) (intrastate) coupling mechanisms.[26,27] Interstate coupling, for example between the Q and B states of metalloporphyrins, is usually weak because the Herzberg–Teller scattering tensor term is divided by the energy separation of the mixing states. For the Q and B states, the separation energy is large; however, for excitation in the weak Q band, the large energy denominator is somewhat offset by the large transition dipole for the Soret, and as a result, the interstate and intrastate couplings can be of about equal magnitudes. Because of the near equivalence of contributions from interstate and intrastate coupling, the A_{2g} modes can become comparable in intensity to the normal modes of other symmetries. On the other hand, excitation into a strong absorption like the Soret band strongly enhances the intrastate contribution but does not affect the interstate contribution. As a result the polarized A_{1g} modes and the depolarized B_{1g} and B_{2g} modes are expected to dominate the spectrum for excitation in the Soret band.[26,27] Strong B_{1g} and B_{2g} mode scattering in the Soret band was predicted[28] and has been observed.[29]

This simple picture of resonance enhancement is complicated in the manganese(III) porphyrins because a number of electronic states that are not involved in more typical metalloporphyrins come into play.[21,30,31] These additional states give rise to the hyper-porphyrin absorption spectrum observed for manganese(III)

(20) Gouterman, M. In *The Porphyrins*; Dolphin, D., Ed.; Academic: New York, 1978; Vol. 3, Chapter 1.
(21) Boucher, L. J. *Coord. Chem. Rev.* **1972**, *7*, 289.
(22) Parthasarathi, N.; Hansen, C.; Yamaguchi, S.; Spiro, T. G. *J. Am. Chem. Soc.* **1987**, *109*, 3865.
(23) Helms, J. H.; ter Haar, L. W.; Hatfield, W. E.; Harris, D. L.; Jayaraj, K.; Toney, G. E.; Gold, A.; Mewborn, T. D.; Pemberton, J. R. *Inorg. Chem.* **1986**, *25*, 2334.

(24) Albrecht, A. C. *J. Chem. Phys.* **1960**, *33*, 156.
(25) Mingardi, M.; Siebrand, W. *J. Chem. Phys.* **1975**, *62*, 1075.
(26) Shelnutt, J. A. *J. Chem. Phys.* **1980**, *72*, 3848.
(27) Shelnutt, J. A. *J. Chem. Phys.* **1977**, *66*, 3387.
(28) See Figure 3, ref 26.
(29) Cheung, L. D.; Yu, N. T.; Felton, R. H. *Chem. Phys. Lett.* **1978**, *55*, 527.
(30) Gouterman, M.; Hanson, L. K.; Khalil, G. E.; Leenstra, W. R. *J. Chem. Phys.* **1975**, *62*, 2343.
(31) Shelnutt, J. A.; O'Shea, D. C.; Yu, N.-T.; Cheung, L. D.; Felton, R. H. *J. Chem. Phys.* **1976**, *64*, 1156.

porphyrins. In particular, the absorption spectra contain extra absorption bands of considerable intensity (Figure 5), and all of the bands are shifted from the positions of typical Q and B bands. For manganese(III) porphyrins the additional states are $\pi \rightarrow$ Mn d_x transitions that have the same symmetry (E_u) as the Q and B bands; consequently, the two charge-transfer transitions mix heavily to give four strong E_u states labeled Q', B', C', and D'.[30,31] These four mixed charge-transfer and $\pi \rightarrow \pi^*$ states can all vibronically couple by the Herzberg–Teller mechanism. Because the interstate vibronic coupling contributions to the Raman line intensity can be cumulative, the presence of additional states to which coupling is possible provides a mechanism for adding intensity to the A_{2g} modes over and above that normally expected from coupling to the B and Q states.[31] The interstate coupling contribution to the Raman line intensities can be further resonanced enhanced if at least one of the additional states is in close proximity (~ 1 vibrational quantum) to the resonant state. And, finally, a D-term[31] interstate coupling contribution becomes important if the Herzberg–Teller state is as close as 1 vibrational quantum above the state at resonance with the exciting light. In this case, the D-term contribution becomes large even for vibronic coupling to a weak electronic state.[31] Such a state (band V_a) has previously been assigned for manganese(III) porphyrin complexes.[21,31] The possible mechanisms contributing to Raman intensities for Mn(III) porphyrins have been treated in detail elsewhere.[31]

From the discussion above it is clear that the appearance of strong A_{2g} (anomalously polarized) modes is not mysterious[22] and, in fact, has been predicted.[31] Strong A_{2g} modes have previously been detected in $Mn^{III}EtioP(NCS)$,[31] $Mn^{III}EtioP(Cl)$,[31] and $Mn^{III}TPP(Cl)$[22,32] for excitation near the bands V and V_a.

Catalytic Oxidation of Cyclohexane with (Tetrakis(2,6-dinitrophenyl)porphinato)manganese(III) and Iodosylbenzene. The catalytic activity of MnTDNPP(Cl) in oxidizing cyclohexane was determined by using gas chromatography to measure product yields. In a typical run, a solution of 4.0 μmol of MnTDNPP(Cl) and 17.6 mg of iodosylbenzene in 1.1 mL of methylene chloride and 0.47 mL of cyclohexane was stirred in a glovebox (argon) for 2 h. A 2-μL injection into the gas chromatograph gave 0.24 μg of cyclohexanone and 1.10 μg of cyclohexanol. Product yields were 1.9 and 8.6 μmol, respectively. Turnover numbers for the 2-h run were 0.5 for cyclohexanone and 2.2 for cyclohexanol; hence, the hydroxylation reaction is catalytic. Total yield was about 13% in terms of oxidant converted to product. A run with MnTPP(Cl) (in benzene) gave about 17% yield, and for MnTF$_5$PP(Cl) the total yield was about 9%. Competing catalytic destruction of iodosylbenzene accounts for the low yields.

Absorption spectra of the MnTDNPP reaction mixture after the run showed the presence of a high-oxidation-state porphyrin intermediate with the Soret band at 424 nm. The intermediate is identified on the basis of its UV–visible spectrum as a Mn(IV) or Mn(V) porphyrin species.[33-38] The reaction had probably not stopped after 2 h. The yield of products was determined at 20-min intervals for 4.5 h during another run with MnTDNPP. After 2 h, the reaction was found to be about 80% complete. By comparison, a similar run with MnTF$_5$PP(Cl) was 90% complete after 2 h. Selectivity for the alcohol (75–85%) over the ketone was similar for MnTDNPP, MnTPP, and MnTF$_5$PP.

Summary

Two metalloporphyrins (TDNPP and TDAPP) with shallow, open cavities adjacent to the central core on both faces of the macrocycle have been synthesized and characterized by UV–visible absorption, proton NMR, FTIR, and resonance Raman spectroscopy. The new porphyrins form the precursors, to which bulky groups can be attached at the ortho positions, to form bis-deep-pocket porphyrins. These porphyrins will possess small pockets adjacent to the central core on both faces of the macrocycle. The cavities can be used to promote binding of small substrate molecules at the metal center and to control the selectivity of reactions at the catalytic site.

During review of this paper, Lindsey and Wagner[39] reported synthesis of ortho-substituted tetraphenylporphyrins, but they were unsuccessful in the synthesis of the di-ortho-substituted nitro derivative and the tetrakis(9-anthracenyl)porphyrin. The procedure used here has also recently been used by us to synthesize the tetrakis(9-anthracenyl)porphyrin.[40] Although we are not sure which of the differences between their procedure and the procedure given here is responsible for our success, we have noted two observations that may be important. First, the reaction times used by us are considerably longer than those used by Lindsey and Wagner. We have noted that the conversion of the porphyrinogen to the porphyrin is very sensitive to the reaction time. For example, the formation of the porphyrin has been followed by UV–visible absorption, and no product is observed after 2 h. Between 4 and 5 h the product yield reaches a maximum, but completely disappears after 6 h. Another important feature is the use of inactive alumina for chromatography. The pure TDNPP is modified during chromatography on Brockman activity 1 alumina to give an unidentified orange compound bound to the column.

The manganese(III) derivative of TDNPP has catalytic activity for converting alkanes to alcohols as shown by the oxidation of cyclohexane. Belova et al. have shown that iron(III) tetrakis(2-nitrophenyl)porphyrin converts methane to methanol at low yield.[41] We have verified that methane and ethane are converted by using instead the Fe derivative of TF$_5$PP.[42] Thus, we may expect similar methane-oxidation activity for the 2,6-dinitro derivative. The tetrakis(2,6-dinitrophenyl)porphyrin derivatives containing Mn and Fe are being investigated to determine the regioselectivity of the alkane hydroxylation reaction.

(32) Gaughan, R. R.; Shriver, D. F.; Boucher, L. J. *Proc. Natl. Acad. Sci. U.S.A.* **1975**, *72*, 433.

(33) Camenzind, M. J.; Hollander, F. J.; Hill, C. L. *Inorg. Chem.* **1982**, *21*, 4301.

(34) Schardt, B. C.; Hollander, F. J.; Hill, C. L. *J. Am. Chem. Soc.* **1983**, *104*, 3964.

(35) Smegal, J. A.; Hill, C. L. *J. Am. Chem. Soc.* **1983**, *105*, 2920.

(36) Smegal, J. A.; Hill, C. L. *J. Am. Chem. Soc.* **1983**, *105*, 3515.

(37) Camenzind, M. J.; Schardt, B. C.; Hill, C. L. *Inorg. Chem.* **1984**, *23*, 1984.

(38) Birchall, T.; Smegal, J. A.; Hill, C. L. *Inorg. Chem.* **1984**, *23*, 1910.

(39) Lindsey, J. S.; Wagner, R. W. *J. Org. Chem.* **1989**, *54*, 828

(40) Quintana, C. A.; Shelnutt, J. A. Unpublished results.

(41) Belova, V. S.; Khenkin, A. M.; Shilov, A. E. *Kinet. Katal.* **1987**, *28*, 1016.

(42) Trudell, D.; Shelnutt, J. A. Unpublished work.